

Assessment and application of electromagnetic induction method to measure Arctic sea ice thickness

GUO Jingxue¹, WANG Huajun^{2*} & SUN Bo¹

¹ Polar Glaciology Division, Polar Research Institute of China, Shanghai 200136, China;

² School of Earth Sciences, Zhejiang University, Hangzhou 310027, China

Received 15 February 2015; accepted 27 July 2015

Abstract The electromagnetic induction method is widely used to measure sea ice thickness. Based on the electrical properties of sea ice and seawater, the method measures the apparent conductivity, which represents the conductivity of the half-space, and calculates the thickness of the sea ice. During the fourth Chinese National Arctic Research Expedition in summer 2010, an integrated electromagnetic induction system was set up on the icebreaker R/V *XUE LONG* to measure sea ice thickness along the ship's tracks to the north of the Chukchi Sea. The conductivities of sea ice, seawater, and brine were measured and a simple forward model was used to explain the effect of changes in those conductivities on the apparent conductivity over a horizontal layered structure. The results of this analysis indicated that when using the electromagnetic induction method to measure sea ice thickness, the conductivity of sea ice could be neglected and the conductivity of seawater could be treated as a constant. The ice distribution results derived from the electromagnetic induction method showed that the typical sea ice thickness was 160 cm and 90 cm during the outbound and the return legs of the voyage, respectively.

Keywords sea ice thickness, electromagnetic induction, forward calculation, conductivity, Arctic

Citation: Guo J X, Wang H J, Sun B. Assessment and application of electromagnetic induction method to measure Arctic sea ice thickness. *Adv Polar Sci*, 2015, 26: 292-298, doi: 10.13679/j.advps.2015.4.00292

1 Introduction

The volume of sea ice in the Polar regions is sensitive to changing climate and therefore serves as an indicator of global climate change. In turn, changes in sea ice affect the climate, and recent rapid changes in the Arctic climate are closely related to changes in the volume of sea ice^[1-3]. The thickness, extent, and concentration of sea ice are all impacted by climate change. For example, the extent of melt pools on the surface of the sea ice and the ratio of open water to ice cover directly influence surface albedo. Therefore, changes in the volume of sea ice can potentially amplify climate change^[1].

Remote sensing methods are widely used to measure the height of the sea ice freeboard and to calculate sea ice

thickness, to measure sea ice extent, and to determine sea ice concentration. Remote sensing data indicate that sea ice thickness, extent, and concentration in the Arctic are decreasing steadily^[4-7]. Comparison of submarine sonar data for the 1970s and 1990s indicates that the average sea ice draft in the central Arctic decreased 40% during that period^[8]. Furthermore, the extent of thick multi-year ice in some parts of the Arctic has been decreasing steadily since 1987^[9]. Remote sensing methods can provide valuable data to evaluate the status of polar sea ice on a large scale. *In situ* measurements of sea ice are important to supplement remote sensing data, and can provide more detailed information than remote sensing methods. For example, *in situ* measurements can provide high-resolution data on snow and ice thickness, melt pools, and sea ice structure.

There have been many studies of sea ice based on *in situ* measurements, from the marginal sea ice zone to transpolar

* Corresponding author (email: wanghj@zju.edu.cn)

regions, from the Arctic to the Antarctic, during summer and winter^[1,10–13]. The physical properties of sea ice vary considerably across and among regions, and it is difficult to obtain fine-scale data. In the Arctic, the sea ice is characterized by its complex structure and differences in thickness across the region^[14]. In recent decades there has been a focus on the development of new technology to measure sea ice thickness on a regional scale. Electromagnetic induction (EMI) is one of the new methods developed to measure sea ice thickness. Research using the EMI method can be conducted from shipboard and airborne platforms and also from the surface of the sea ice^[15–19].

This study investigated the EMI method in terms of the theory underlying the calculations. A calculation model was developed and the accuracy of the final statistical ice thickness distributions was assessed based on shipboard observations. Changes in the apparent conductivity caused by changes in the conductivity of sea ice, seawater, and brine were also investigated. This work offers new insights into the effectiveness of the EMI method to measure sea ice thickness at a regional scale, and demonstrates why the conductivity of sea ice can be neglected, why the conductivity of seawater can be regarded as constant, and why the accuracy of the EMI method is poor in the deformed ice zone.

2 Working principles of the EMI method

The EM31 conductivity meter is the most commonly used instrument to measure sea ice thickness based on the EMI theory. The instrument consists of a transmitter coil and receiver coil that function as magnetic dipole antennas, and can be operated in vertical or horizontal dipole mode (Figure 1). The spacing between the coplanar transmitter and receiver antenna coils is 3.66 m and the fixed operating frequency is 9.8 kHz.

First, we assume that the instrument is operated in the vertical dipole mode, which corresponds to the normal orientation of the instrument. The primary field is generated as the current is injected into the transmitter coil. When the receiver coil is coplanar with the transmitter coil the primary field (a quasi-static low-frequency electromagnetic field) can be written as follows:

$$H_{z,p} = -\frac{M}{4\pi r^3}, \quad (1)$$

where M is the transmitted magnetic moment and r is the spacing between the transmitter and receiver coils. When the

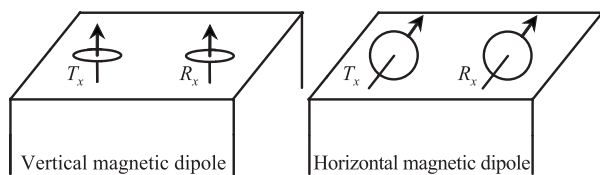


Figure 1 Schematic of the EM31 electromagnetic induction instrument showing the transmitter (T_x) and receiver (R_x) coils operating in vertical and horizontal dipole mode.

primary magnetic field interacts with electrical conductors in the half-space below the equipment, eddy currents are induced. These eddy currents result in a secondary magnetic field, which adds to the primary field and is sensed by the receiver coil. The in-phase component and the quadrature component measured by the electromagnetic instrument are the real and imaginary parts of the ratio, respectively, between the secondary field and the primary field, while the secondary field is the value of the measured total field minus the primary field. Therefore, the secondary field can be written as follows:

$$H_{z,s} = H_z - H_{z,p} = (iQ + I)H_{z,p}, \quad (2)$$

where H_z is the measured total field in the medium, $H_{z,p}$ is the primary field in the medium, Q is the quadrature component, and I is the in-phase component. The EM31 instrument records only the quadrature component and represents it as the apparent conductivity as follows:

$$\sigma_a = \frac{4Q}{2\pi f \mu_0 r^2}, \quad (3)$$

where f is the operating frequency, μ_0 is the magnetic permeability of the free space, and r is the spacing between the transmitter and receiver coils.

The apparent conductivity represents the integrated conductivity of the half-space and is measured in $\text{mS}\cdot\text{m}^{-1}$. For the measurement of sea ice thickness, the apparent conductivity is a function of the conductivities of sea ice and seawater and the height above the sea ice and the seawater. Seawater conductivity can be considered constant within a certain area, and the contribution of sea ice conductivity can be neglected relative to seawater conductivity. Therefore, the apparent conductivity mainly depends on the height of the instrument above the surface of the seawater, which is the underside of the sea ice.

The distance from the instrument to the underside of the sea ice (the ice–sea interface) can be calculated based on apparent conductivity, and the height of the instrument above the surface of the sea ice is determined using a sonar altimeter and a laser altimeter. The two altimeters are used to ensure the quality and accuracy of the data. The sea ice thickness is then obtained by the subtraction of the two heights.

3 Field measurements

During the fourth Chinese National Arctic Research Expedition (4th CHINARE-Arctic) in summer 2010, the EM31 instrument (Geonics Ltd) was operated in vertical dipole mode from the icebreaker R/V *XUE LONG* to measure sea ice thickness along the ship's outbound and return tracks to the north of the Chukchi Sea (Figure 2). The measurement system included an EM31-MK2 electromagnetic induction instrument, a SR50A sonar altimeter (Campbell Ltd), an LDM42 laser altimeter (Jenoptik Ltd), and a global positioning system (GPS) sensor. For observations, the measurement system was suspended below the bow of the icebreaker to minimize the influence

of magnetic material such as the ship’s hull. The height above the ice was about 3 m and the distance to the hull was about 7 m. The data were recorded while the icebreaker was travelling through sea ice. In addition, sea ice thickness was measured using the EM31 measurement system on the surface of the sea ice. These measurements combined with measurements obtained from sea ice drilling were used to determine the accuracy of the shipboard data.

The shipboard observations were performed from 28 July to 30 August 2010. During the observations, the icebreaker was travelling through the sea ice at about 3 m·s⁻¹, and the specified recording interval for the measurement system was 1 s. Therefore, each data point corresponded to a horizontal distance of 3 m in the ice field. The EM31 data represent the average conductivity over a range of about 4 m, and provide an estimation of sea ice thickness.

To overcome the limitation imposed by the harsh environment of the polar regions, an integrated EMI sea ice thickness monitoring system was developed. The system enabled cooperative control of multiple sensors including an EMI instrument, sonar altimeter, laser altimeter, and GPS sensor. In addition, the system included wireless data transmission and graphic monitoring technology so the data from the sensor suspended from the bow of the ship could be sent to the interior control unit and monitoring unit in real time. This integrated structure ensured convenient, safe, and reliable operation of the EMI system.

4 Forward analysis of the conductivity response

As mentioned in section 2, apparent conductivity mainly depends on the height of the measurement system above the ice–sea interface. However, several factors can influence the conductivity response, including the components and

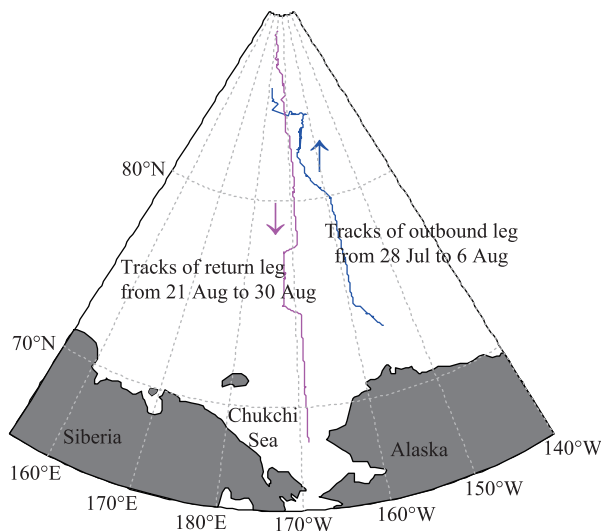


Figure 2 Location of the Arctic sea ice zone where sea ice thickness was measured using the shipboard EM31 system. The blue line indicates the outbound leg of the voyage and the pink line indicates the return leg.

structure of the sea ice and the properties of the seawater. In the present study, three parameters were investigated using forward calculation analysis to explain the effect of these parameters on the apparent conductivity response. A simple two-layered forward model was used to calculate the EMI responses over a horizontal layered structure of sea ice and seawater. In line with the working principles of the EMI method, the transmitter coil in the EMI instrument transmitted a current signal that passed through the medium and was received by the receiver coil. Because the diameter of the coils is much less than the distance between them, they can be regarded as a magnetic dipole. The more complex four-layered forward geoelectric model incorporating the sea ice layer, brine layer, and seawater layer is shown in Figure 3. Equation (4) is the formula used to calculate the relative anomalies of the vertical magnetic dipole in the frequency

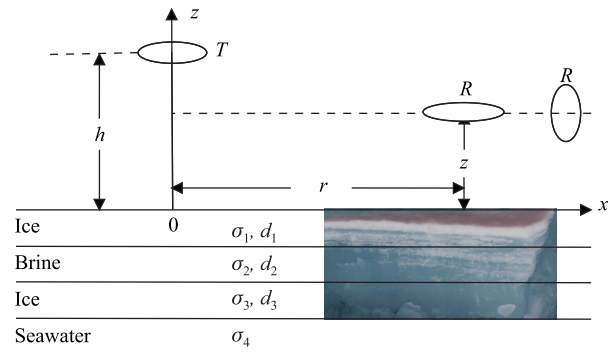


Figure 3 Schematic of the forward layered geoelectric model.

domain.

$$H_{abn} = \frac{H_{z,s}}{H_{z,p}} \approx -r^3 \int_0^\infty r_{TE} e^{-2\lambda h} \lambda^2 J_0(\lambda r) d\lambda, \quad (4)$$

where $H_{z,s}$ is the secondary field in the medium and $H_{z,p}$ is the primary field in the medium, r is the inter-coil space (3.66 m for the EM31 instrument), h is the height of the instrument above the sea ice, J_0 is a zero-order Bessel function, λ is an integral variable, and r_{TE} is the total reflection coefficient of the underground medium. The recursive formula for r_{TE} can be represented as follows:

$$r_{TE} = \frac{u_0 - u^{(1)}}{u_0 + u^{(1)}}, \quad (5)$$

where $u^{(i)}$ is surface admittance, which can be obtained from the following formula:

$$u^{(i)} = u_i \frac{u^{(i+1)} + u_i \tanh(u_i d_i)}{u_i + u^{(i+1)} \tanh(u_i d_i)}, \quad (i = n-1, n-2, \dots, 1), \quad (6)$$

$$u^{(n)} = u_n, \quad (7)$$

where u_i is the characteristic admittance of the i layer, and d_i is the layer’s thickness. u_i is calculated as follows:

$$u_i = \sqrt{\lambda^2 - k_i^2}, \quad (8)$$

where k_i is the complex wave number of the i layer, which

can be expressed as:

$$k_i^2 = -\mu_i s(\varepsilon_i s + \sigma_i), \quad (i=1, 2, \dots, n), \quad (9)$$

where μ_i , ε_i , and σ_i represent the magnetic permeability, dielectric constant, and conductivity, respectively, and s is the Laplace variable:

$$s = j\omega = j2\pi f, \quad (10)$$

where ω is the circular frequency, and f is the operating frequency (9.8 kHz for the EM31 instrument). The EMI method actually uses H_{abn} (the ratio of the secondary field in the medium $H_{z,s}$ and the primary field in the medium $H_{z,p}$) to detect sea ice thickness and records the quadrature component, which is sensitive to conductivity. The quadrature component can then be used to calculate the apparent conductivity using equation (3). The apparent conductivity is a function of the operating frequency, system height, thickness, and the actual conductivity (σ_i).

The observation mode was set to vertical dipole mode, the same as the EM31 instrument. The height of measurement system above the sea ice can also influence the results, so the height was set at 2 m, 3 m, and 4 m, to determine which height provides results consistent with actual measurements^[20]. Sea ice conductivity is also a significant variable across different regions. Therefore, strictly speaking it is inappropriate to neglect sea ice conductivity. The effect of the finite sea ice conductivity on the calculated thickness was investigated to clarify why the influence of sea ice conductivity is not normally considered, and to determine the error range resulting from the exclusion of sea ice conductivity from the calculation.

According to previous data, the range of sea ice conductivity was set at 0–30 $\text{mS}\cdot\text{m}^{-1}$ ^[18], the sea ice thickness was set at 1.5 m, and seawater conductivity was set at a constant 2500 $\text{mS}\cdot\text{m}^{-1}$. Figure 4 shows the apparent conductivity response to changes in sea ice conductivity from 0–30 $\text{mS}\cdot\text{m}^{-1}$ at the three heights above the sea ice. The apparent conductivity was calculated from numeric parameters using three fitting formulas. For example, for measurements made at a height of 4 m above the sea ice, the calculated apparent conductivity corresponding to sea ice conductivity of 30 $\text{mS}\cdot\text{m}^{-1}$ and 0 $\text{mS}\cdot\text{m}^{-1}$ was 54.3 $\text{mS}\cdot\text{m}^{-1}$ and 53.3 $\text{mS}\cdot\text{m}^{-1}$, respectively. Therefore, the relative error caused by neglecting the conductivity of sea ice at a thickness of 1.5 m was 1.8% or 2.7 cm.

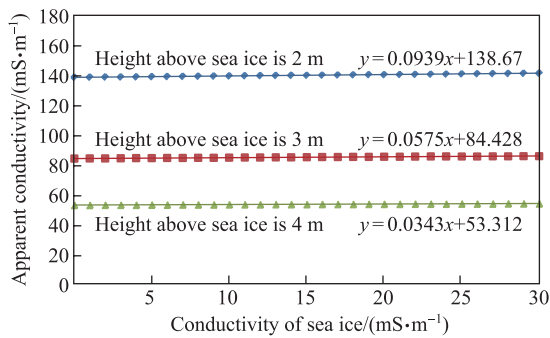


Figure 4 Apparent conductivity response to changes in sea ice conductivity.

For measurements at heights of 3 m and 2 m above the sea ice, the relative error was 2.1% (about 3 cm) and 2% (3 cm), respectively.

The same method was used to investigate the effect of seawater conductivity on the calculated sea ice thickness. Although seawater conductivity varies on a global scale, it can be regarded as a constant across a polar region.

For this analysis, the range of seawater conductivity was set at 2000–3000 $\text{mS}\cdot\text{m}^{-1}$, the sea ice thickness was set at 1.5 m, and sea ice conductivity was set at a constant 10 $\text{mS}\cdot\text{m}^{-1}$. Figure 5 shows the apparent conductivity response to changes in seawater conductivity from 2000–3000 $\text{mS}\cdot\text{m}^{-1}$ at the three heights above the sea ice. Again, the apparent conductivity was calculated from numeric parameters using three fitting formulas. For example, for measurements made at a height of 4 m above the sea ice, the calculated apparent conductivity corresponding to seawater conductivity of 2000 $\text{mS}\cdot\text{m}^{-1}$ and 3000 $\text{mS}\cdot\text{m}^{-1}$ was 53.3 $\text{mS}\cdot\text{m}^{-1}$ and 53.8 $\text{mS}\cdot\text{m}^{-1}$, respectively. Therefore, the relative error caused by treating seawater conductivity as a constant was 1% at a sea ice thickness of 1.5 m or about 1.5 cm. For measurements at heights of 3 m and 2 m above the sea ice, the relative error was 3.2% (about 4.7 cm) and 5.2% (about 7.8 cm), respectively.

As reported in a number of previous studies^[18–19], the accuracy of the EMI method is expected to decrease over deformed ice. For this reason, the brine content in the sea ice should be considered as well as the influence of pressure ridges. Different to the two-layer models used to calculate the effect of changes in sea ice and seawater conductivity, a brine layer was added to generate a four-layered forward model to investigate the impact of changes in brine conductivity on measurements of sea ice thickness (Figure 3).

Because it is difficult to measure brine conductivity directly, the brine conductivity was assumed to be in the range of 0–2000 $\text{mS}\cdot\text{m}^{-1}$ to represent seawater inflow, and the brine layer thickness was set at 0.2 m. Sea ice conductivity was set at 10 $\text{mS}\cdot\text{m}^{-1}$, sea ice thickness at 1.5 m, and seawater conductivity at 2500 $\text{mS}\cdot\text{m}^{-1}$. The apparent conductivity response and the fitting formulas are shown in Figure 6. For measurements made at a height of 4 m, the calculated apparent conductivity corresponding to brine conductivity

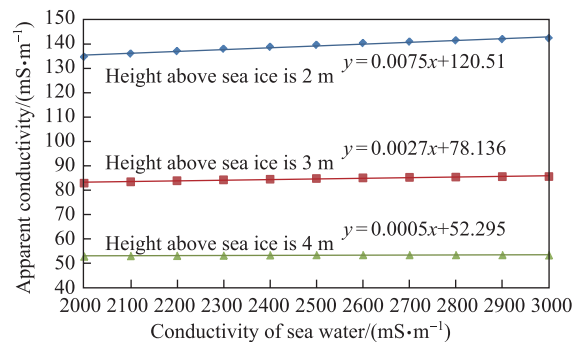


Figure 5 Apparent conductivity response to changes in seawater conductivity.

of 0 mS·m⁻¹ and 2000 mS·m⁻¹ was 49.2 mS·m⁻¹ and 59.4 mS·m⁻¹, respectively. Therefore, the relative error related to brine conductivity was about 17.2% (25.8 cm) for a sea ice thickness of 1.5 m. For measurements made at heights of 3 m and 2 m, the relative error was about 18.2% (about 27.3 cm) and 18.4% (27.5 cm), respectively.

The effect on the apparent conductivity differed considerably for the three parameters investigated. Table 1 lists the confluence for the results of the three forward models and the relative error. The relative error related to changes in sea ice conductivity was very small. The relative error related to changes in seawater conductivity was also small. This is consistent with the hypothesis that sea ice conductivity can be neglected relative to seawater conductivity and that seawater conductivity can be considered constant within a certain area. However, as shown in Table 1 and Figure 6 the relative error caused by the brine conductivity was considerable, indicating that the accuracy of sea ice thickness measured using the EMI method could be poor over deformed ice with high brine content. The error means that the thickness of sea ice measured by the EMI method will be less than the actual thickness.

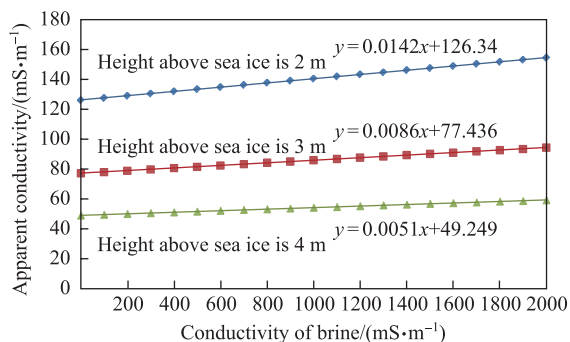


Figure 6 Apparent conductivity response to changes in brine conductivity.

5 Calculation of sea ice thickness

In the research process, there are two ways to obtain the height of the measurement system above seawater. One way is to measure the apparent conductivity and then convert the apparent conductivity to obtain the height above the ice–sea interface. The other is to apply the EM31-ICE module (provided by the manufacturer) to measure the height above the ice–sea interface directly.

To ensure accurate thickness results, in the present study the apparent conductivity was converted from the measured conductivity. To determine the accuracy of this method, the apparent conductivity was measured as the equipment height was gradually increased over open water. The conversion formula can be derived based on exponential fit as follows:

$$H = 12.74 - 1.87 * \log(\sigma_a - 12.02), \tag{11}$$

where H is the height in meters. The forward calculation curve (vertical dipole mode) shown in Figure 7 can be used to compare the calculated and the measured values. Due to the influence of the hull, the two curves have the same tendency but not overlap. Equation (11) is used to calculate changes in the height of the measurement system across the observation profile and the sea ice thickness is obtained by subtraction. Visual observations confirmed that level rather than deformed sea ice was predominant along the ship’s tracks. Therefore, sea ice conductivity was neglected and seawater conductivity was considered as constant for the analysis of sea ice thickness.

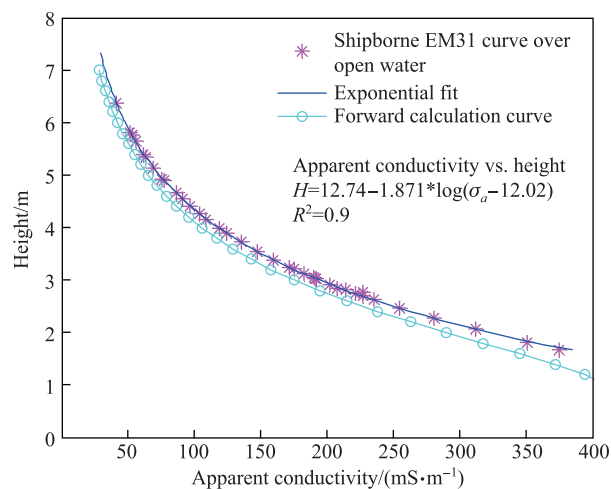


Figure 7 The relationship between apparent conductivity and the height of the measurement system above seawater.

6 Field data examples

To produce the calculated sea ice thickness profile shown in Figure 8, 260 consecutive observed data points were selected. From this subset of the data it can be seen that the sea ice thickness was relatively constant at around 1 m, but with occasional ice ridges 4–5 m thick.

Table 1 Apparent conductivity response based on the forward calculation model

Height /m	Effect of sea ice conductivity			Effect of sea water conductivity			Effect of brine conductivity		
	Min. / (mS·m ⁻¹)	Max. / (mS·m ⁻¹)	Relative error	Min. / (mS·m ⁻¹)	Max. / (mS·m ⁻¹)	Relative error	Min. / (mS·m ⁻¹)	Max. / (mS·m ⁻¹)	Relative error
4	53.3	54.3	1.8%	53.3	53.8	1.0%	49.2	59.4	17.2%
3	84.4	86.2	2.1%	83.5	86.2	3.2%	77.4	94.6	18.2%
2	138.7	141.5	2.0%	135.5	143.0	5.2%	126.3	154.7	18.4%

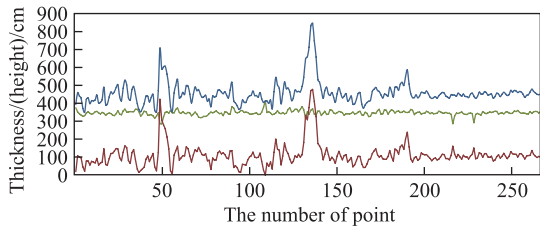


Figure 8 Subsample of data from the shipborne profiles (260 consecutive data points 3 m apart). The blue line indicates the height above the ice–sea interface measured by the EM31 instrument. The green line indicates the height above the surface of the sea ice measured by the laser altimeter. The red line indicates the sea ice thickness obtained by subtraction of the two sets of data.

Xie et al.^[21] have previously reported the preliminary results of sea ice thickness measured using the EMI method during the 4th CHINARE-Arctic. The present report presents the final interpretation of the results following analysis of anomalous data with wavelet domain denoising and statistical processing^[22]. The histograms in Figure 9 show the sea ice thickness distributions for the outbound and return tracks shown in Figure 2.

Sea ice thickness distributions describe the state of the sea ice and can be used in the analysis of sea ice mass budget and dynamic–thermodynamic processes and potentially to construct an ice morphology model to better understand the ice thickness distribution^[23]. The EMI method provides accurate and reliable measurements of sea ice thickness. The sea ice during the outbound leg of the voyage was thicker than that during the return leg. The peaks at 160 cm and 30 cm represent the typical sea ice thickness during the outbound leg and the peak at 90 cm represents the typical sea ice thickness during the return leg. Both distributions have long tails to the right with maximum thicknesses of more than 400 cm. The difference in the peak sea ice thickness between the two legs of the voyage was likely caused by the different melting characteristics of first-year and multi-year ice. The two peaks for the outbound leg indicate that both first-year ice and multi-year ice were present on the outbound track from the end of July to early August. The single peak for the return leg indicates that only multi-year ice was present on the return track in late August because the first-year ice had melted. Therefore, the difference in the number of peaks reflects the characteristics and speed of ice melting.

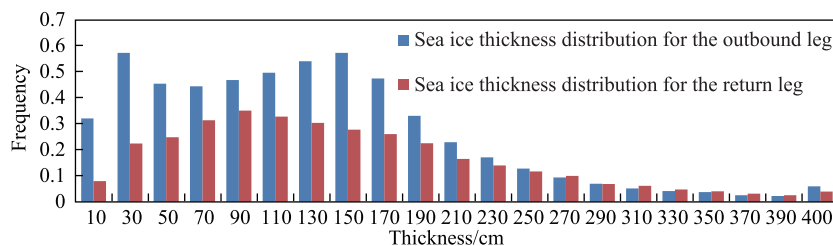


Figure 9 Sea ice thickness distributions for the outbound leg (blue) and the return leg (red) of the 4th CHINARE-Arctic.

7 Conclusions and discussions

The EMI method is invaluable technology to detect sea ice thickness distribution. The method provides a reliable and efficient means to obtain high quality data on sea ice thickness at local and regional scales. In the present study, shipboard measurements and forward theoretical calculations were used to assess the accuracy and applicability of the EMI method to measure sea ice thickness, and to obtain ice thickness distribution data for the tracks of the R/V *XUE LONG* during the 4th CHINARE-Arctic. The EM31 system cannot accurately measure the thickness of deformed ice^[3]. This was proven in the present analysis using the forward calculation model, which demonstrated that brine in the ice is an important factor in terms of conductivity.

The apparent conductivity measured using the EMI method represents the average conductivity over a volume. Therefore, the method can be used to estimate the average thickness of the sea ice below the equipment, but the accuracy of the results will be less than that for results obtained using sea ice drilling. However, this does not impact on the practical value of the EMI method to measure sea ice thickness. The formula for the conversion from the measured apparent conductivity to the height of measurement system was obtained through a specific experiment based on changing the height of the measurement system over open water. Many previous studies have shown that this method can be used to obtain accurate sea ice thickness, but the formulas derived from different height measurements differ considerably. This probably reflects different research vessels and study locations with different electrical properties of the local seawater and different sea ice structure. More research is needed to ensure that the method can be applied with high accuracy over various locations.

Finally, to improve the precision and reliability of sea ice measurements and the theoretical methods used to calculate sea ice thickness, more complex equivalent multi-layer sea ice forward calculation models are needed. These models should consider the complex physical structure of sea ice including overlying snow, fusion infiltration layers, brine layers, and air bubbles. Differences in conductivity between first-year ice and multi-year ice also need to be taken into account. Whereas the conductivity of sea ice is currently considered to be constant within a certain area, the target of future models to calculate sea ice thickness should be to treat the sea ice as a complex, multi-layered, and non-homogeneous structure.

Acknowledgments This work was supported by the National Natural Science Foundation of China (Grant no. 41006116), the National Major Scientific Research Project (Grant no. 2013CBA01804), and the Chinese Polar Environmental Comprehensive Investigation and Assessment Programs (Grant no. CHINARE-2015-02-02).

References

- 1 Perovich D K, Grenfell T C, Light B, et al. Transpolar observations of the morphological properties of Arctic sea ice. *J Geophys Res*, 2009, 114(C00A04), doi: 10.1029/2008JC004892
- 2 Wei L X, Zhang Z H. Analysis of Arctic sea ice variability. *Marine Forecasts*, 2007, 24(4): 42–48 (in Chinese)
- 3 Worby A P, Griffin P W, Lytle V I, et al. On the use of electromagnetic induction sounding to determine winter and spring sea ice thickness in the Antarctic. *Cold Reg Sci Technol*, 1999, 29(1): 49–58
- 4 Comiso J C, Parkinson C L, Gersten R, et al. Accelerated decline in the Arctic sea ice cover. *Geophys Res Lett*, 2008, 35(L01703), doi: 10.1029/2007GL031972
- 5 Nghiem S V, Rigor I G, Perovich D K, et al. Rapid reduction of Arctic perennial sea ice. *Geophys Res Lett*, 2007, 34(L19504), doi: 10.1029/2007GL031138
- 6 Stroeve J C, Serreze M C, Fetterer F, et al. Tracking the Arctic's shrinking ice cover: Another extreme September minimum in 2004. *Geophys Res Lett*, 2005, 32(L04501), doi: 10.1029/2004GL021810
- 7 Parkinson C L, Cavalieri D J, Gloersen P, et al. Arctic sea ice extents, areas, and trends 1978–1996. *J Geophys Res*, 1999, 104(C9): 20837–20856
- 8 Lindsay R, Schweiger A. Arctic sea ice thickness loss determined using subsurface, aircraft, and satellite observations. *Cryosphere*, 2015, 9: 269–283
- 9 Tucker W B III, Weatherly J W, Eppler D T, et al. Evidence for rapid thinning of sea ice in the western Arctic Ocean at the end of the 1980s. *Geophys Res Lett*, 2001, 28(14): 2851–2854
- 10 Tucker W B III, Gow A J, Weeks W F. Physical properties of summer sea ice in the Fram Strait. *J Geophys Res*, 1987, 92(C7): 6787–6803
- 11 Martinson D G, Steele M. Future of the Arctic sea ice cover: Implications of an Antarctic analog. *Geophys Res Lett*, 2001, 28(2): 307–310
- 12 Haas C. Late-summer sea ice thickness variability in the Arctic Transpolar Drift 1991–2001 derived from ground-based electromagnetic sounding. *Geophys Res Lett*, 2004, 31(L09402), doi: 10.1029/2003GL019394
- 13 Haas C, Gerland S, Eicken H, et al. Comparison of sea-ice thickness measurements under summer and winter conditions in the Arctic using a small electromagnetic induction device. *Geophysics*, 1997, 62(3): 749–757
- 14 Winsor P. Arctic sea ice thickness remained constant during the 1990s. *Geophys Res Lett*, 2001, 28(6): 1039–1041
- 15 Haas C, Hendricks S, Eicken H, et al. Synoptic airborne thickness surveys reveal state of Arctic sea ice cover. *Geophys Res Lett*, 2010, 37(L09501), doi: 10.1029/2010GL042652
- 16 Reid J E, Pfaffling A, Worby A P, et al. In situ measurements of the direct-current conductivity of Antarctic sea ice: implications for airborne electromagnetic sounding of sea-ice thickness. *Ann Glaciol*, 2006, 44(1): 217–223
- 17 Haas C, Lobach J, Hendricks S, et al. Helicopter-borne measurements of sea ice thickness, using a small and lightweight, digital EM system. *J Appl Geophys*, 2009, 67(3): 234–241
- 18 Haas C. Evaluation of ship-based electromagnetic-inductive thickness measurements of summer sea-ice in the Bellingshausen and Amundsen seas, Antarctica. *Cold Reg Sci Technol*, 1998, 27(1): 1–16
- 19 Reid J E, Worby A P, Urbancich J, et al. Shipborne electromagnetic measurements of Antarctic sea-ice thickness. *Geophysics*, 2003, 68(5): 1537–1546
- 20 Guo J X, Sun B, Tian G, et al. Research on electromagnetic inductive measurement of sea-ice thickness in Antarctic Prydz Bay. *Chinese J Geophys*, 2008, 51(2): 419–426(in Chinese)
- 21 Xie H, Lei R, Ke C, et al. Summer sea ice characteristics and morphology in the Pacific Arctic sector as observed during the CHINARE 2010 cruise. *Cryosphere*, 2013, 7(4): 1057–1072
- 22 Wang J, Guo J X, Wang H J, et al. Data analysis of shipborne EM31-ice measuring in the fourth Chinese National Arctic Research Expedition. *Chinese J Polar Res*, 2012, 24(1): 47–52(in Chinese)
- 23 Multala J, Hautaniemi H, Oksama M, et al. An airborne electromagnetic system on a fixed wing aircraft for sea ice thickness mapping. *Cold Reg Sci Technol*, 1996, 24(4): 355–373